Bioorganic Chemistry 52 (2014) 1–7

Contents lists available at ScienceDirect

Bioorganic Chemistry

journal homepage: www.elsevier.com/locate/bioorg

Design, synthesis, molecular docking studies and *in vitro* screening of ethyl 4-(3-benzoylthioureido) benzoates as urease inhibitors

Aamer Saeed [a], Muhammad Siraj Khan [b], Hummera Rafique [c], Mohammad Shahid [d], Jamshed Iqbal [b,*]

[a] Department of Chemistry, Quaid-I-Azam University, Islamabad, Pakistan
[b] Department of Pharmaceutical Sciences, COMSATS Institute of Information Technology, Abbottabad 22060, Pakistan
[c] Department of Chemistry, University of Gujrat, Gujrat 50700, Pakistan
[d] Fraunhofer Institute SCAI, Department of Bioinformatics, Germany

ARTICLE INFO

Article history:
Received 16 July 2013
Available online 30 October 2013

Keywords:
Antioxidant activity
Ethyl 4-(3-benzoylthioureido)benzoates
Molecular docking
Urease inhibition

ABSTRACT

Thioureas are exceptionally versatile building blocks towards the synthesis of wide variety of heterocyclic systems, which also possess extensive range of pharmacological activities. The substituted benzoic acids were converted into corresponding acid chlorides, these acid chlorides were then treated with potassium thiocyanate in acetone and then the reaction mixture was refluxed for 1–2 h afford ethyl 4-(3-benzoylthioureido)benzoates thioureas in good yields. All the newly synthesized compounds were evaluated for their urease inhibitory activities and were found to be potent inhibitors of urease enzyme. Compounds **1f** and **1g** were identified as the most potent urease inhibitors (IC_{50} 0.21 and 0.13 μM, respectively), and was 100-fold more potent than the standard inhibitors. Further molecular docking studies were carried out using the crystal structure of urease to find out the binding mode of the inhibitors with the enzyme.

1. Introduction

Urease (EC 3.5.1.5; urea amidohydrolase) is a metal containing enzyme that catalyzes the hydrolysis of urea into ammonia and carbamates [1,2]. Ureases are widespread in nature among plants, bacteria, fungi, algae and invertebrates. Urease producing bacteria have a harmful effect on human health. In humans the urease of *Helicobacter pylori* causes infections of gastrointestinal and urinary tract [3], such as stomach cancer and the peptic ulcer [4]. Other urease associated diseases include hepatic encephalopathy, urolithiasis, urinary catheter encrustation, pyelonephritis and hepatic coma [5]. *H. pylori* survive at the low pH of stomach during colonization, which ultimately leads to gastric and peptic ulcers and, in some cases it may lead to cancer [6]. Strategies based on urease inhibition are the major treatment of diseases caused by *H. pylori* and associated urease producing bacteria. Ureases are inhibited by different classes of compounds [7]. Thioureas and their derivatives [8,9] were found to have a significant inhibitory activity against the urease enzyme. Thioureas attracted worldwide attention due to their number of applications and diverse biological significance, possess a wide range of biological applications including antiviral, antibacterial, antifungal, antitubercular, antithyroidal, herbicidal, insecticidal activities and they act as agrochemicals [10–12]. 1-Benzoyl-3-(4,6-disubstituted)pyrimidine-2-yl-thioureas have excellent herbicidal activities. Some acylthioureas have been found to possess pesticidal effects and it also promotes plant growth [10]. Halo-thiophene and pyridyl substituted heterocyclic thioureas are inhibitors of non-nucleoside HIV-1 reverse transcriptase [13,14]. Various thiourea derivatives act as potential neuraminidase inhibitors of influenza virus [15]. Some thioureas have been shown to have notable positive effect on the germination of maize seeds as well as on the chlorophyll contents in seedling leaves. Thioureas serve as well-known chelating agents for transition metals complexes [16]. *N*,*N*-Dialkyl-*N*′-benzoylthioureas act as selective complexing agents for the enrichment of platinum metals even from strongly interfering matrixes [17].

The complexes of thiourea derivatives also show broad spectrum of biological activities. High stability and simple synthesis made it possible to use the *N*-benzoylthiourea group as modifier of silica for complexation gas chromatography. By taking the advantage of the chelating properties of *N*-benzoylthioureas Cu(II) ions were bonded with silica to give a packing π-type interaction with absorbates having electron donor properties [18]. The high selectivity of this packing permitted the separation of complex mixtures including isomers of different classes of organic compounds. Silica was chemically modified with *N*-acyl-*N*′-benzoylthiourea group. The resulting material was observed to behave as a selective mean of preconcentration of Cd(II), Zn(II) and Cu(II) from ethanol fuel by means of column technique. Ethanolic solutions having 6

* Corresponding author. Fax: +92 992 383441.
E-mail address: drjamshed@ciit.net.pk (J. Iqbal).

0045-2068/$ - see front matter © 2013 Elsevier Inc. All rights reserved.
http://dx.doi.org/10.1016/j.bioorg.2013.10.001

micro mol of the metal ion were percolated through the column and retention of 100% were achieved for all metals [19]. *N*-(substituted-phenyl)-*N*-phenylthioureas have been developed as anion-binding site in a hydrogen-bonding receptors, calyx, arenes containing thioureas as neutral receptors towards α,α-dicarboxylate anions [20]. Benzoylthiourea of general formula (R—NH(C=S)—NH)$_n$—Z where R = alkyl, cycloalkyl, aryl, alkenyl, etc. and Z is aromatic ring are used in the optical recording medium which is heat resistance, plasticizer resistant, moisture resistance and water resistance. Thiourea derivatives serves as precursors and are important intermediate involved in the synthesis of a variety of heterocyclic systems with wide range of biological and synthetic applications i.e. iminothiazolidinones, thiohydantoins, imidazole-2-thiones, thiazolines, thiazolamines, etc. [21,22].

In the present study, ethyl 4-(3-benzoylthioureido) benzoate derivatives were synthesized and evaluated for urease inhibitory activity. The obtained results showed high activity of the synthesized thiourea derivatives with IC_{50} of 0.13 μM for the most potent compound. The binding mode of the compounds was predicted by molecular docking studies. Moreover, the compounds were tested against 1,1-diphenyl-2-picrylhydrazyl (DPPH) radical scavenging activities.

2. Results and discussion

2.1. Chemistry

The substituted benzoic acids were converted into corresponding acid chlorides by their reaction with thionyl chloride. These acid chlorides were then treated with potassium thiocyanate in acetone and then reaction mixture was refluxed with 1–2 h afforded aminoethylbenzoate to afford 1-aroyl-3-(*p*-ethylbenzoato)thioureas, which were further purified by recrystallization from ethanol. The synthetic pathway is illustrated in Scheme 1.

In the IR spectra, the characteristic absorptions for the N—H protons of ethyl 4-(3-benzoylthioureido) benzoates (**1a–j**) appeared in the range of 3298–3332 cm^{-1}. The ester carbonyl carbon absorption peaks observed at 1722–1729 cm^{-1}and the amidic carbonyl absorption appeared at 1671–1688 cm^{-1}.

The synthesis of ethyl 4-(3-benzoylthioureido) benzoates (**1a–j**) was also confirmed by ^{1}H NMR due to the presence of a two characteristic broad band singlet for —NH protons at δ 11.31–11.42 ppm and another —NH peak observed at δ 10.23–10.38 ppm. In ^{13}C NMR spectra the characteristics carbonyl carbon peaks of ester moeity observed in the range of δ 165.4–166.2 ppm and amide carbonyl carbon appeared at δ 167.2–168.2 ppm. The (C=S) carbon signal appeared in the range of δ 180.4–181.2 ppm. Mass spectroscopy and elemental analysis of ester thioureas also confirm their synthesis successfully. General structure for the series of compounds synthesized is as below.

2.2. Urease inhibition assay

All of the newly synthesized ethyl 4-(3-benzoylthioureido) benzoate derivatives were found to be potent inhibitors of urease of *Canavalia ensiformis* (Table 1). Compounds **1f** and **1g** were the most potent compounds among the series with IC_{50} = 0.21 and 0.13 μM, respectively. Compound **1f** having mono methoxy was slightly less potent than **1g** having di methoxy groups as a substituent. All of the investigated compounds were 100-fold more than active than the positive controls, thiourea (IC_{50} = 20.3 μM) and acetohydroxamic acid (IC_{50} = 43.2 μM). Halogenated substituted thiourea derivatives were slightly less active than methoxy substituted compounds. In brief, the compounds having electron donating (—OCH_3) substituents were slightly more potent inhibitors than electron withdrawing substituents (—Cl or —F).

2.3. Antioxidant activity assay

Thiourea derivatives and their metal complexes had shown significant antioxidant activity [23–25]. Most of the investigated ethyl 4-(3-benzoylthioureido) benzoate derivatives showed good antioxidant activities (Table 1). Compounds **1a**, **1b**, **1c**, **1d**, **1f** and **1j** with IC_{50} values 4.13, 4.98, 4.10, 1.93, 2.17 and 7.16 μM, respectively. The ethyl 4-(3-benzoylthioureido) benzoate derivatives have the ability to donate hydrogen when reacted with DPPH radical to form radical hybrid, like thiosemicarbazones [26]. Propyl gallate and 2-tert-butyl-4-hydroxyanisole were used as reference standards in the antioxidant assay. The tested compounds were more potent antioxidant as compared to reference standards, except compounds **1e** and **1h**. Compound **1d** (IC_{50} = 1.93 μM) was the most potent compound with methyl group as substituent showing good antioxidant activity even at very low concentrations.

2.4. Docking and pose ranking

The results of re-docking experiment showed that the enzyme structure and its binding site were well prepared and the docking program reproduced the natively bound conformations of the co-crystallized bound ligand. The docking results for the compounds **1a–1j** were achieved, which showed that there were different conformations (poses) predicted for each compound. Table 2 shows the docking scores obtained with FlexX and the rank number of best pose obtained with NNScore [27] algorithm for the compounds screened against the enzyme. Docking scores of the compounds range between −12 and −24 kcal/mol, however, filtering the poses for the compounds by NNScore showed there could be other conformations that might interact favorably with the enzymes. With the exception of two compounds (**1b** and **1d**), the difference in the docking scores for the first docking pose and the predicted favorable pose for all compounds was approximately

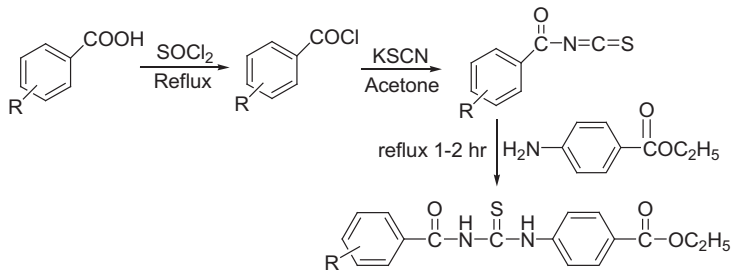

R = H, 3-Cl, 2,4-Dichloro, 4-CH_3, 3-CH_3, 4-OCH_3, 3,4-Dimethoxy, 3-OCH_3,2-Br, 2-F.

Scheme 1. Ethyl 4-(3-benzoylthioureido) benzoates (**1a–j**).

Table 1
Urease inhibition and antioxidant activity of the compounds (**1a–1j**).

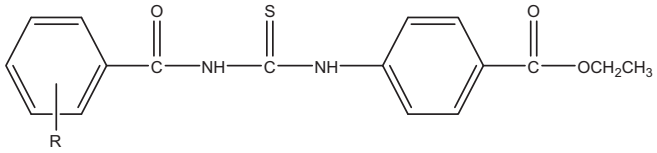

Compounds	R	Urease inhibition IC_{50} (μM) ± SEM	Antioxidant IC_{50} (μM) ± SEM or %
1a	H	0.51 ± 0.071	4.13 ± 0.06
1b	3-Cl	0.26 ± 0.032	4.98 ± 0.27
1c	2,4-diCl	0.28 ± 0.23	4.10 ± 0.49
1d	4-CH_3	0.67 ± 0.19	1.93 ± 0.18
1e	3-CH_3	1.07 ± 0.12	27.9 ± 2.15%
1f	4-OCH_3	0.21 ± 0.48	2.17 ± 0.01
1g	3,4-diOCH_3	0.13 ± 0.061	12.8 ± 1.06
1h	2-Br	0.35 ± 0.015	12.8 ± 1.3%
1i	2-OCH_3	0.47 ± 0.053	14.5 ± 0.36
1j	2-F	0.73 ± 0.059	7.16 ± 0.41
Thiourea		20.3 ± 5	–
AHA		43.2 ± 2.6	–
PG		–	24 ± 3
TBH		–	27.6 ± 2.1

– Not determined, AHA, acetohydroxamic acid, PG, n-propyl gallate, TBH, 2-tert-butyl-4-hydroxyanisole.

Table 2
Docking scores and best pose ranks for the compounds docked against the urease enzyme.

Compound	Docking scores (kcal/mol)	Pose ranks in top 10	Docking score for selected pose
1a	−16.60	3	−14.62
1b	−17.13	9	−10.82
1c	−12.51	2	−10.41
1d	−13.59	8	−9.38
1e	−17.48	7	−14.68
1f	−24.56	2	−22.99
1g	−20.52	2	−20.18
1h	−13.11	6	−12.07
1i	−14.64	5	−13.20
1j	−15.40	9	−12.17

2 kcal/mol. For the two compounds, a larger difference of approximately 4–6 kcal/mol was observed.

The docked poses of all compounds are shown in Fig. 1. It has been observed that the top ranked selected poses with high predicted activity of all compounds interact within the active site of the enzyme in a similar way. The strict pharmacophoric criterion is not fulfilled during the docking calculations, because no docking predictions were made when the strict metal pharmacomphore constraints were specified. However, when the two metal pharmacophore criteria was relieved and set to optional, interaction with one of the two nickel atoms was observed. The oxygen atom in benzoic acid moiety of all compounds interacts with the second nickel atom. The same oxygen atom is involved in hydrogen bonding interaction with His492 in the active site. Another hydrogen bond interaction is observed between the amine nitrogen and Asp494. These three interactions are common in all the predicted poses of the compounds. Aromatic interactions of the benzene ring with two alanine residues (Ala440 and Ala636) and Met637 are formed which helps in tightly holding the compounds towards the nickel center in the active site. However, the predicted conformation of **1f** is compound is opposite as compared to other compounds, in which the oxygen atom in the phenyl moiety make interactions with the nickel atom and His494.

The calculated docking scores of the first predicted poses of each compound show a small correlation of 0.28 with the activity values, however, the correlation is slightly increased to 0.33 if the docking scores of the selected poses are used. It is unlikely to observer a good correlation of the docking scores with the activity values because of the limitations in the scoring functions of the docking programs. For this purpose, more rigorous methods such as molecular dynamics followed by molecular mechanics based free energy of binding calculation would be required. However, a bottleneck in using such sophisticated methods is the time consuming and compute expensive charge derivation methods.

2.5. Binding mode analysis

A common binding mode was observed for the compounds docked to the urease enzyme. The hydrophobic opening of urease pocket is composed of several hydrophobic residues that include Ala440, Asp494, Aala636, and Met637. As shown in the interaction diagrams in Figs. 2 and 3, the aromatic ring of the benzoic acid moiety of all compounds form hydrophobic interactions with these residues. Aromatic interactions are also formed between the phenyl tail of the compounds and the above mentioned hydrophobic residues as well as two histidine residues (His492 and His519) that are located in the entrance of the enzyme active site. His492 is also involved in making hydrogen bonds with the carboxyl oxygen. The preferred binding modes selected by the external scoring function are resulting in a binding mode that is favored by most of the compounds except the compounds **1f** and **1g**. **1f** and **1g** adapt conformations that are flipped opposite with respect to the conformations of all other compounds. Both of these compounds form hydrogen bonds with Arg439. Although, in all cases, all the compounds interacts with only one metal atom and adapt conformations where the oxygen of the compound occupies the middle of both nickel atoms.

3. Experimental

3.1. General

^{1}H NMR were recorder on a Brucker AM-300 spectrophotometer and chemical shifts of ^{1}H NMR are reported in parts per million (ppm). The melting point was determined on Staurt SMP3 melting point apparatus and is uncorrected. FTIR spectra were recorded using Shimadzu IR 460 spectrophotometer by Attenuated Total Reflectance (ATR) method. The elemental analysis was performed on LECO-932 CHNS analyzer.

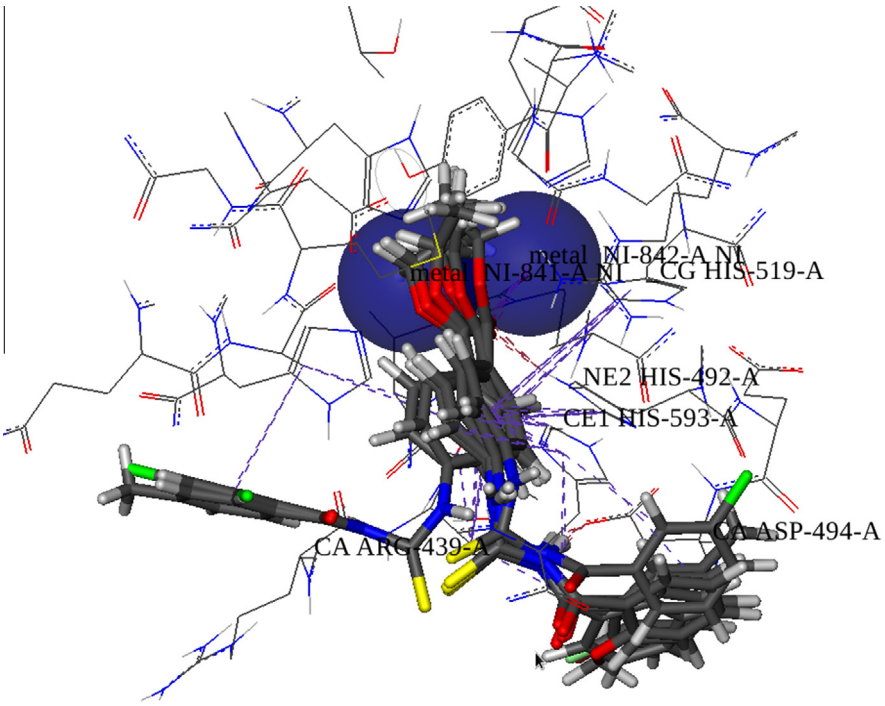

Fig. 1. Predicted docked poses of the compounds inside the active site of urease enzyme. The docked conformations of the compounds are shown in stick representation and the two nickel atoms are represented by blue spheres. Hydrogen bonding and aromatic interactions with the surrounding residues are shown with dotted lines. (For interpretation of the references to color in this figure legend, the reader is referred to the web version of this article.)

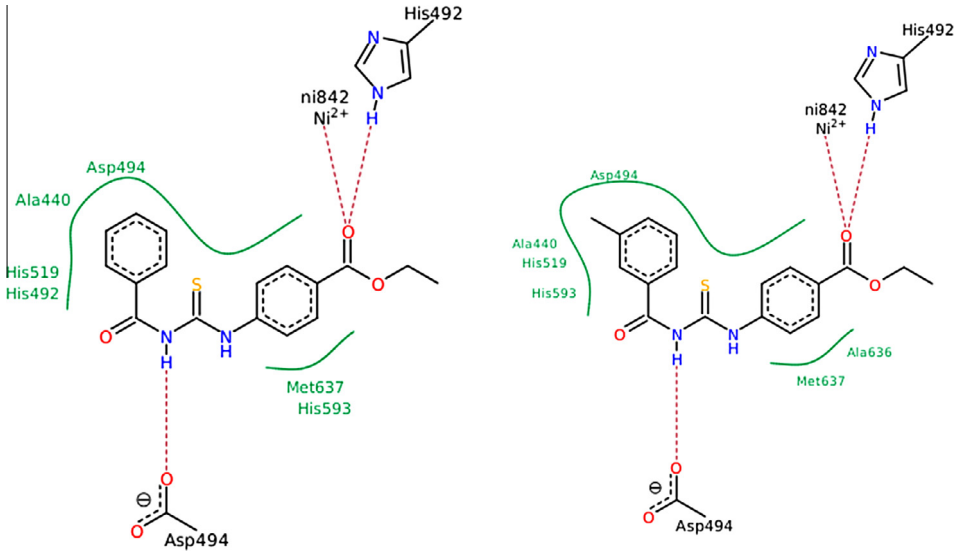

Fig. 2. Interaction diagrams for compounds **1a** and **1e**. Hydrogen bond and metal interactions are shown with dotted lines. Green lines represent the hydrophobic residues located in the active site. (Left): interaction diagram of compound **1a** showing interactions with active site residues. (Right): interaction diagram of **1e** showing interactions with active site residues. (For interpretation of the references to color in this figure legend, the reader is referred to the web version of this article.)

*3.2. Synthesis of ethyl 4-(3-benzoylthioureido) benzoates (1**a–j**)*

Variously substituted benzoic acids (0.02 mol) were treated with 2 mL (1.3 eq) of thionylchloride through a dropping funnel and the reaction mixture was heated under reflux for 2–3 h yields corresponding acid chlorides. To a stirred solution of potassium thiocyanate (1.2 g, 0.02 mol) in 10 mL dry acetone, placed in round bottom flask fitted with a reflux condenser. (1.5 mL, 0.02 mol) of freshly prepared acid chlorides was added drop wise. After the initial reaction had subsided a solution of ethyl 4-animobenzoate (0.02 mol) in acetone (20 mL) was added slowly with constant stirring followed by reflux for 1–2 h. The mixture was poured into crushed ice when the ethyl 4-(3-benzoylthioureido) benzoates **(1a–j)** precipitated as solid. The solid product was filtered, then dried and recrystallized from suitable solvent.

*3.2.1. Ethyl 4-(3-benzoylthioureido) benzoate (**1a**)*

Yield = 74%; Rf^a = 0.8; M.P. = 140–142 °C; IR (KBr) ν_{max}: 3298 (N—H), 1724 (ester C=O), 1675 (amide C=O), 1583 (C=C), 1272 (C=S), 1152 (C—N) cm^{-1}; ^1H NMR ($CDCl_3$, δ ppm): 11.31 (1H, s, —NH), 10.24 (1H, s, —NH), 7.92 (1H, d, *J* = 7.8 Hz, H-2,H-6), 7.56–7.87 (5H, m, Ar), 7.47 (1H, d, *J* = 7.8 Hz, H-3,H-5), 4.21 (2H, q,

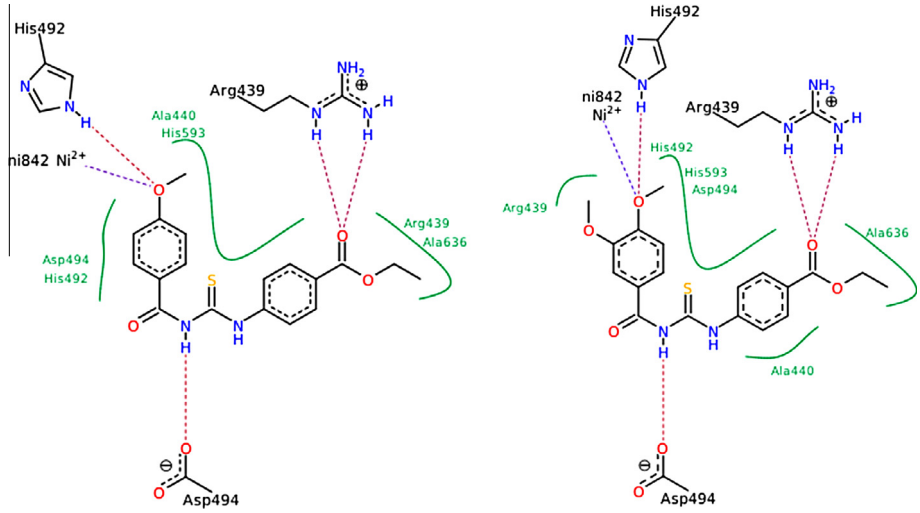

Fig. 3. Interaction diagrams for compounds **1f** and **1g**. Hydrogen bond and metal interactions are shown with dotted lines. Green lines represent the hydrophobic residues located at the opening of the active site. (Left): interaction diagram of compound **1f** showing interactions with active site residues. (Right): Interaction diagram of **1g** showing interactions with active site residues. (For interpretation of the references to color in this figure legend, the reader is referred to the web version of this article.)

J = 7.2 Hz, —CH_2), 2.21 (3H, t, *J* = 5.6 Hz, —CH_3); ^{13}C NMR ($CDCl_3$, δ ppm): 180.4 (C=S), 167.3 (amide C=O), 165.4 (ester C=O), 138.6 (C-4), 135.4 (C-1'), 132.6 (C-4'), 130.5 (C-2,C-6), 129.4 (C-3',C-5'), 128.7 (C-2',C-6'), 127.6 (C-3,C-5), 126.7 (C-1), 60.2 (—OCH_2), 14.3 (—CH_3); EIMS (70 eV): *m*/*z* (%); [M^+] 328 (42%); Anal. Calcd for $C_{17}H_{16}N_2O_3S$; C, 62.19; H, 4.88; N, 8.54; S, 9.76. Found: C, 62.11; H, 4.64; N, 8.33; S, 9.54.

3.2.2. Ethyl 4-[3-(3-chlorobenzoyl)thioureido]benzoate (**1b**)

Yield = 78%; Rf[a] = 0.7; M.P. = 156–158 °C; IR (KBr) ν_{max}: 3302 (N—H), 1727 (ester C=O), 1673 (amide C=O), 1578 (C=C), 1280 (C=S), 1153 (C—N) cm^{-1}; ^{1}H NMR ($CDCl_3$, δ ppm): 11.37 (1H, s, —NH), 10.32 (1H, s, —NH), 7.95 (1H, d, *J* = 7.8 Hz, H-2,H-6), 7.84 (1H, d, *J* = 2.4 Hz, H-2'), 7.76 (1H, d, *J* = 7.4 Hz, H-6'), 7.66 (1H, d, *J* = 7.8 Hz, H-3,H-5), 7.58 (1H, dd, *J* = 7.2,2.4 Hz, H-4'), 7.49 (1H, dd, *J* = 7.2,7.4 Hz, H-5'), 4.26 (2H, q, *J* = 7.2 Hz, —CH_2), 2.26 (3H, t, *J* = 5.6 Hz, —CH_3); ^{13}C NMR ($CDCl_3$, δ ppm): 180.8 (C=S), 167.5 (amide C=O), 165.6 (ester C=O), 138.7 (C-4), 136.4 (C-1'), 135.5 (C-3'), 133.7 (C-4'), 130.7 (C-2,C-6), 129.4 (C-5'), 128.5 (C-2'), 127.4 (C-3,C-5), 126.5 (C-1), 125.8 (C-6'), 60.3 (—OCH_2), 14.2 (—CH_3); EIMS (70 eV): *m*/*z* (%); [M^+] 362.5 (53%); Anal. Calcd for $C_{17}H_{15}N_2O_3SCl$; C, 56.27; H, 4.14; N, 7.72; S, 8.83. Found: C, 56.14; H, 4.06; N, 7.53; S, 8.64.

3.2.3. Ethyl 4-[3-(2,4-dichlorobenzoyl)thioureido]benzoate (**1c**)

Yield = 80%; Rf[a] = 0.75; M.P. = 117–118 °C; IR (KBr) ν_{max}: 3309 (N—H), 1723 (ester C=O), 1678 (amide C=O), 1586 (C=C), 1283 (C=S), 1157 (C—N) cm^{-1}; ^{1}H NMR ($CDCl_3$, δ ppm): 11.42 (1H, s, —NH), 10.38 (1H, s, —NH), 7.97 (1H, d, *J* = 7.8 Hz, H-2,H-6), 7.86 (1H, d, *J* = 2.3 Hz, H-3'), 7.78 (1H, d, *J* = 7.2 Hz, H-6'), 7.67 (1H, dd, *J* = 7.2,2.3 Hz, H-5'), 7.54 (1H, d, *J* = 7.8 Hz, H-3,H-5), 4.27 (2H, q, *J* = 7.2 Hz, —CH_2), 2.28 (3H, t, *J* = 5.6 Hz, —CH_3); ^{13}C NMR ($CDCl_3$, δ ppm): 181.2 (C=S), 167.8 (amide C=O), 166.2 (ester C=O), 139.5 (C-4), 138.4 (C-4'), 135.2 (C-2'), 132.3 (C-3'), 131.7 (C-1'), 130.8 (C-6'), 130.3 (C-2,C-6), 128.1 (C-5'), 127.2 (C-3,C-5), 126.8 (C-1), 60.8 (—OCH_2), 14.5 (—CH_3); EIMS (70 eV): *m*/*z* (%); [M^+] 397 (37%); Anal. Calcd for $C_{17}H_{14}N_2O_3SCl_2$; C, 51.38; H, 3.53; N, 7.05; S, 8.06. Found: C, 51.27; H, 3.35; N, 6.93; S, 7.93.

3.2.4. Ethyl 4-[3-(4-methylbenzoyl)thioureido]benzoate (**1d**)

Yield = 71%; Rf[a] = 0.7; M.P. = 223–224 °C; IR (KBr) ν_{max}: 3329 (N—H), 1726 (ester C=O), 1681 (amide C=O), 1584 (C=C), 1286 (C=S), 1154 (C—N) cm^{-1}; ^{1}H NMR ($CDCl_3$, δ ppm): 11.34 (1H, s, —NH), 10.27 (1H, s, —NH), 7.88 (1H, d, *J* = 7.8 Hz, H-2,H-6), 7.77 (1H, d, *J* = 7.4 Hz, H-2',H-6'), 7.68 (1H, d, *J* = 7.8 Hz, H-3,H-5), 7.57 (1H, d, *J* = 7.4 Hz, H-3',H-5'), 4.24 (2H, q, *J* = 7.2 Hz, —CH_2), 2.62 (3H, s, Ar—CH_3), 2.25 (3H, t, *J* = 5.6 Hz, —CH_3); ^{13}C NMR ($CDCl_3$, δ ppm): 180.6 (C=S), 167.5 (amide C=O), 165.4 (ester C=O), 138.7 (C-4), 137.8 (C-4'), 132.6 (C-1'), 131.4 (C-2,C-6), 130.3 (C-3',C-5'), 128.2 (C-2',C-6'), 127.6 (C-3,C-5), 126.7 (C-1), 60.4 (2H, s, —OCH_2), 24.3 (Ar—CH_3), 14.4 (—CH_3); EIMS (70 eV): *m*/*z* (%); [M^+] 342 (61%); Anal. Calcd for $C_{18}H_{18}N_2O_3S$; C, 63.16; H, 5.26; N, 7.02; S, 9.36. Found: C, 63.07; H, 5.14; N, 6.95; S, 9.21.

3.2.5. Ethyl 4-[3-(3-methylbenzoyl)thioureido]benzoate (**1e**)

Yield = 78%; Rf[a] = 0.7; M.P. = 196–198 °C; IR (KBr) ν_{max}: 3322 (N—H), 1722 (ester C=O), 1671 (amide C=O), 1588 (C=C), 1284 (C=S), 1156 (C—N) cm^{-1}; ^{1}H NMR ($CDCl_3$, δ ppm): 11.35 (1H, s, —NH), 10.31 (1H, s, —NH), 7.86 (1H, d, *J* = 7.8 Hz H-2,H-6), 7.75 (1H, d, *J* = 7.2 Hz, H-6'), 7.66 (1H, d, *J* = 2.4 Hz, H-2'), 7.58 (1H, dd, *J* = 7.4,7.2 Hz, H-5'), 7.53 (1H, dd, *J* = 7.4,2.4 Hz, H-4'), 7.46 (1H, d, *J* = 7.8 Hz, H-3,H-5), 4.23 (2H, q, *J* = 7.2 Hz, —CH_2), 2.61 (3H, s, Ar—CH_3), 2.24 (3H, t, *J* = 5.6 Hz, —CH_3); ^{13}C NMR ($CDCl_3$, δ ppm): 180.5 (C=S), 167.6 (amide C=O), 165.7 (ester C=O), 138.9 (C-4), 137.8 (C-3'), 134.5 (C-1'), 133.2 (C-4'), 130.5 (C-2,C-6), 129.3 (C-5'), 128.2 (C-2'), 127.1 (C-3,C-5), 126.4 (C-1), 125.4 (C-6'), 60.5 (-OCH_2), 24.1 (Ar—CH_3), 14.3 (—CH_3); EIMS (70 eV): *m*/*z* (%); [M^+] 342 (53%); Anal. Calcd for $C_{18}H_{18}N_2O_3S$; C, 63.15; H, 5.25; N, 7.01; S, 9.35. Found: C, 63.08; H, 5.17; N, 6.94; S, 9.24.

3.2.6. Ethyl 4-[3-(4-methoxybenzoyl)thioureido]benzoate (**1f**)

Yield = 76%; Rf[a] = 0.65; M.P. = 207–208 °C; IR (KBr) ν_{max}: 3315 (N—H), 1726 (ester C=O), 1674 (amide C=O), 1587 (C=C), 1282 (C=S), 1165 (C—N) cm^{-1}; ^{1}H NMR ($CDCl_3$, δ ppm): 11.38 (1H, s, —NH), 10.29 (1H, s, —NH), 7.86 (1H, d, *J* = 7.8 Hz, H-2,H-6), 7.73 (1H, d, *J* = 7.5 Hz, H-2',H-6'), 7.64 (1H, d, *J* = 7.5 Hz, H-3',H-5'), 7.54 (1H, d, *J* = 7.8 Hz, H-3,H-5), 4.27 (2H, q, *J* = 7.2 Hz, —CH_2), 3.72 (3H, s, —OCH_3), 2.25 (3H, t, *J* = 5.6 Hz, —CH_3); ^{13}C NMR ($CDCl_3$, δ ppm): 180.6 (C=S), 167.4 (amide C=O), 165.5 (ester C=O), 139.6 (C-4'), 138.5 (C-4), 134.5 (C-1'), 130.7 (C-2,C-6), 129.5 (C-2',C-6'), 127.2 (C-3,C-5), 126.7 (C-1), 117.4 (C-3',C-5'), 60.6 (—OCH_2), 56.5 (Ar-OCH_3), 14.2 (—CH_3); EIMS (70 eV): *m*/*z* (%); [M^+] 358 (46%); Anal. Calcd for $C_{18}H_{18}N_2O_4S$; C, 60.33; H, 5.03; N, 6.70; S, 8.94. Found: C, 60.27; H, 4.92; N, 6.58; S, 8.86.

*3.2.7. Ethyl 4-[3-(3,4-dimethoxybenzoyl)thioureido]benzoate (**1g**)*

Yield = 72%; Rf[a] = 0.6; M.P. = 232–234 °C; IR (KBr) ν_{max}: 3321 (N—H), 1724 (ester C=O), 1678 (amide C=O), 1585 (C=C), 1267 (C=S), 1147 (C—N) cm^{-1}; ^1H NMR, ($CDCl_3$, δ ppm): 11.40 (1H, s, —NH), 10.32 (1H, s, —NH), 7.90 (1H, d, *J* = 7.8 Hz, H-2,H-6), 7.84 (1H, d, *J* = 7.4 Hz, H-6'), 7.73 (1H, d, *J* = 7.8 Hz, H-3,H-5), 7.65 (1H, s, Ar-H-2'), 7.56 (1H, d, *J* = 7.5 Hz, H-5'), 4.27 (2H, q, *J* = 7.2 Hz, —CH_2), 3.78 (3H, s, 3-OCH_3), 3.75 (3H, s, 4-OCH_3), 2.25 (3H, t, *J* = 5.6 Hz, —CH_3); ^{13}C NMR ($CDCl_3$, δ ppm): 180.7 (C=S), 167.7 (amide C=O), 165.8 (ester C=O), 139.8 (C-4'), 138.7 (C-3'), 137.6 (C-4), 130.8 (C-2,C-6), 128.3 (C-1'), 127.1 (C-3,C-5), 126.5 (C-1), 121.6 (C-6'), 117.4 (C-5'), 115.5 (C-2'), 60.6 (—OCH_2), 56.5 (Ar—OCH_3), 14.2 (—CH_3); EIMS (70 eV): *m*/*z* (%); [M^+] 388 (33%); Anal. Calcd for $C_{19}H_{20}N_2O_5S$; C, 58.76; H, 5.15; N, 6.18; S, 8.25. Found: C, 58.57; H, 5.09; N, 6.11; S, 8.17.

*3.2.8. Ethyl 4-[3-(2-bromobenzoyl)thioureido]benzoate (**1h**)*

Yield = 74%; Rf[a] = 0.67; M.P. = 213–215 °C; IR (KBr) ν_{max}: 1728 (ester C=O), 3317 (N—H), 1683 (amide C=O), 1576 (C=C), 1262 (C=S), 1165 (C—N) cm^{-1}; ^1H NMR ($CDCl_3$, δ ppm): 11.34 (1H, s, —NH), 10.23 (1H, s, —NH), 7.85 (1H, d, *J* = 7.8 Hz, H-2,H-6), 7.63–7.81 (4H, m, Ar), 7.56 (1H, d, *J* = 7.8 Hz, H-3,H-5), 4.23 (2H, q, *J* = 7.2 Hz, —CH_2), 2.26 (3H, t, *J* = 5.6 Hz, —CH_3); ^{13}C NMR ($CDCl_3$, δ ppm): 180.4 (C=S), 167.2 (amide C=O), 165.6 (ester C=O), 138.6 (C-4), 137.5 (C-1'), 135.4 (C-4'), 132.7 (C-3'), 131.2 (C-2,C-6), 130.5 (C-6'), 128.4 (C-5'), 127.3 (C-3,C-5), 126.8 (C-1), 121.4 (C-2'), 60.4 (—OCH_2), 14.3 (—CH_3); EIMS (70 eV): *m*/*z* (%); [M^+] 406 (46%); Anal. Calcd for $C_{17}H_{15}N_2O_3SBr$; C, 50.25; H, 3.69; N, 6.90; S, 7.88. Found: C, 50.17; H, 3.56; N, 6.76; S, 7.74.

*3.2.9. Ethyl 4-[3-(3-methoxybenzoyl)thioureido]benzoate (**1i**)*

Yield = 73%; Rf[a] = 0.6; M.P. = 173–174 °C; IR (KBr) ν_{max}: 1725 (ester C=O), 3325 (N—H), 1685 (amide C=O), 1581 (C=C), 1264 (C=S), 1148 (C—N) cm^{-1}; ^1H NMR ($CDCl_3$, δ ppm): 11.36 (1H, s, —NH), 10.27 (1H, s, —NH), 7.87 (1H, d, *J* = 7.8 Hz, H-2,H-6), 7.57–7.77 (4H, m, Ar), 7.53 (1H, d, *J* = 7.8 Hz, H-3,H-5), 4.25 (2H, q, *J* = 7.2 Hz, —CH_2), 3.73 (3H, s, —OCH_3), 2.26 (3H, t, *J* = 5.6 Hz, —CH_3); ^{13}C NMR ($CDCl_3$, δ ppm): 180.5 (C=S), 167.6 (amide C=O), 165.7 (ester C=O), 138.7 (C-3'), 137.6 (C-4), 134.2 (C-4'), 131.3 (C-2,C-6), 129.1 (C-6'), 127.4 (C-3,C-5), 126.6 (C-1), 122.5 (C-5'), 118.4 (C-1'), 116.5 (C-2'), 60.7 (—OCH_2), 56.4 (Ar-OCH_3), 14.5 (—CH_3); EIMS (70 eV): *m*/*z* (%); [$M^{+\cdot}$] 358 (54%); Anal. Calcd for $C_{18}H_{18}N_2O_4S$; C, 60.34; H, 3.02; N, 6.70; S, 8.93. Found: C, 60.23; H, 4.93; N, 6.53; S, 8.81.

*3.2.10. Ethyl 4-[3-(2-fluorobenzoyl)thioureido]benzoate (**1j**)*

Yield = 68%; Rf[a] = 0.7; M.P. = 123–124 °C; IR (KBr) ν_{max}: 1729 (ester C=O), 3332 (N—H), 1688 (amide C=O), 1591 (C=C), 1271 (C=S), 1156 (C—N) cm^{-1}; ^1H NMR ($CDCl_3$, δ ppm): 11.42 (1H, s, —NH), 10.34 (1H, s, —NH), 7.93 (1H, d, *J* = 7.8 Hz, H-2,H-6), 7.64–7.89 (4H, m, Ar), 7.58 (1H, d, *J* = 7.8, Hz H-3,H-5), 4.26 (2H, q, *J* = 7.2 Hz, —CH_2), 2.28 (3H, t, *J* = 5.6 Hz, —CH_3); ^{13}C NMR ($CDCl_3$, δ ppm): 181.4 (C=S), 168.2 (amide C=O), 166.5 (ester C=O), 140.6 (C-2'), 138.7 (C-4), 134.7 (C-4'), 131.2 (C-2,C-6), 129.3 (C-6'), 127.3 (C-3,C-5), 126.7 (C-1), 126.3 (C-1'), 125.6 (C-5'), 117.6 (C-3'), 61.2 (—OCH_2), 14.8 (—CH_3); EIMS (70 eV): *m*/*z* (%); [M^+] 346 (24%); Anal. Calcd for $C_{17}H_{15}N_2O_3SF$; C, 58.96; H, 4.34; N, 6.94; S, 9.25. Found: C, 58.87; H, 4.21; N, 6.73; S, 9.12.

3.3. Assay for urease inhibition

The *in vitro studies* were carried out for the synthesized compounds by testing them against the jack bean urease. The enzyme activity was determined by measuring the absorbance and quantification of ammonia was done by using the indophenols method as described by Weatherburn [28]. In brief, the assay mixture contained 40 μL of buffer (0.01 M $LiCl_2$, 1 mM EDTA, 0.01 M K_2HPO_4, pH 8.2) containing 100 mM urea, 10 μL of enzyme (*Canavalia ensiformis*, 5 U/mL) and 10 μL of the test compound. The assay mixture was incubated at 37 °C for 10 min in a 96-wellplate. A 40 μL of alkali reagent (0.5%, w/v NaOH, 0.1% active chloride NaOCl) and 40 μL of the phenol reagents (1%, w/v phenol, 0.005%, w/v sodium nitroprusside) were then added to the each well. The absorbance was measured at 625 nm by using microplate reader (Bio-TekELx 800™, Instruments, Inc. USA). Percentage inhibition was calculated using the formula 100 − (OD test well/OD control) × 100. The IC_{50} values were determined by using PRISM 4.0 (GraphPad, San Diego, California, USA).

3.4. Antioxidant assay

The free radical scavenging capacity of the compounds was measured by 1,1-diphenyl-2-picrylhydrazyl (DPPH) methods described by Choudhary et al. with some modification [29]. The assay involved the reaction of the test compounds with 1,1-diphenyl-2-picrylhyrazyl free radical. The reaction was carried out for 30 min at 37 °C with 100 mM DPPH. Decrease in absorbance was measured at 515 nm using micro plate reader (Bio-TekELx 800™, Instruments, Inc. USA). Percent RSA (radical scavenging activity) was determined for the samples using a DMSO treated control group in comparison. The following equation was used for calculation of RSA (%) = 100 − {(OD test well/OD control) × 100}.

3.5. Structure selection and preparation for docking studies

Molecular docking studies were conducted to observe the interactions and selectivity of the compounds against urease enzyme. The three dimensional, high-resolution structure of urease enzyme (PDB Code: 3LA4) was selected from the Protein Data Bank and prepared for molecular modeling. The X-ray structure has well defined binding site, as the crystal structure of the enzyme is co-crystallized with a bound ligand.

Before studying the enzyme in molecular modeling experiment, the enzyme structure was prepared. The structure was protonated with Protonate3D [30] algorithm implemented in the molecular modeling tool MOE [31]. Missing atoms of some residues were completed with utility programs built-in in AmberTools-1.5 package [32]. However, the missing residues were not added because they are far away from the binding site. Accurate charge derivation for such a metal complex is much time consuming and requires expensive computations if quantum mechanical optimization methods are used. Therefore, before minimization process, +2 charges were assigned to the both nickel atoms present in the active site of the urease. It was made sure that the modified residues are not excluded during structure preparation. The carbamylated lysine and methylated cysteine residues were retained as such. The structure was energy minimized using Amber 99 force field with all the heteroatoms and solvent molecules present in the enzyme structure in MOE environment. The backbone atoms were restrained with a small force constant of 100 in order to avoid collapse of the binding pockets during energy minimization calculations. The force field based energy minimization algorithms were used which includes steepest decent followed by conjugate gradient optimization methods. An RMS gradient of 0.05 was specified that would terminate the energy minimization process if the root mean square gradient falls below 0.05. After minimization, the co-crystallized ligands and other solvent molecules were removed before performing docking calculations.

3.6. Preparation of compounds

The 3D structural coordinates of the compounds were generated for all the compounds using MOE followed by assignment of protonation and ionization states in physiological pH range by using the "wash" module. Afterwards, the compounds structures were energy minimized with MMFF94x force field for screening them against the urease enzyme by docking.

3.7. Docking studies

The docking calculations were performed by FlexX [33] docking engine inside the molecular modeling tool LeadIT [34]. For the docking studies, the binding site of the enzyme was defined by including the surrounding amino acid residues around 7.5 Å radius of the co-crystallized bound ligand. The metal atoms were also included in the binding pocket definition. The modified carboxylated LYS residue (KCX490) and methylated CYS residue (CME207) were retained in the structure during docking calculations. Pharmacophoric constraints were defined for the two metal atoms. The constraints were selected to be first essential and then optional to check if the interactions with the metals will be predicted during the docking calculations. The default docking and scoring parameters were chosen for the docking calculations and the top 10 docked conformations were retained for analyzing the interactions and binding modes of individual compounds. In order to make sure that the protein structure is prepared well for docking, the co-crystallized bound ligand was re-docked to reproduce the crystal structure's binding mode.

3.8. Pose ranking and selection

The docked poses of each compound were evaluated for favorable interactions with the enzyme and predicted poses for each docked compound were evaluated by using an external scoring function NNScore. NNScore is a neural network based scoring function that evaluates and predicts the activity for the most favorable conformation (pose) among a set of different poses for the same molecule. The predicted poses for each compound were exported to Mol2 format by the docking program and converted to PDBQT format as required as input by the NNScore program. The conversion to PDBQT was performed by using scripts available in MGL Tools. Similarly, the enzyme PDB structure was also converted to PDBQT format. The poses for each compound were ranked on the basis of the predicted activity values and the top ranked pose of each compound with high activity was selected for visual analysis.

4. Conclusion

An efficient synthesis of some ethyl 4-(3-benzoylthioureido) benzoate thioureas has been carried out, which possess significant antiurease and antioxidant activities. Compounds **1f** and **1g** showed significant activity against the urease. The docking studies conducted on the urease, it can be concluded that the predicted binding poses that are filtered by the external scoring function results in interactions that are observed in most of the compounds. Two possible binding modes can be observed in the predicted docked conformations, however, the interactions and their orientation in the active site pocket of the enzyme remains the same. The identified thiourea derivatives can be utilized in further optimization of biological activity using structural variations in the main skeleton. The antioxidant activity of most of the compounds was more than the standard drugs. Therefore, the investigated radical scavengers can be further evaluated *in vivo* for their efficacy to prevent or control the oxidative stress in diseased models.

Acknowledgment

This work was financially supported by COMSTECH–TWAS and German-Pakistani Research Collaboration Programme.

References

[1] H. Mobley, R. Hausinger, Microbiol. Rev. 53 (1989) 85–108.
[2] P.A. Karplus, M.A. Pearson, R.P. Hausinger, Acc. Chem. Res. 30 (1997) 330–337.
[3] C.M. Collins, S.E. D'Orazio, Mol. Microbiol. 9 (1993) 907–913.
[4] C. Montecucco, R. Rappuoli, Nat. Rev. Mol. Cell Biol. 2 (2001) 457–466.
[5] M. Hanif, M. Saleem, M.T. Hussain, N.H. Rama, S. Zaib, M.A.M. Aslam, P.G. Jones, J. Iqbal, J. Braz. Chem. Soc. 23 (2012) 854–860.
[6] H.L. Mobley, M.D. Island, R.P. Hausinger, Microbiol. Rev. 59 (1995) 451–480.
[7] B. Krajewska, J. Mol. Catal. B: Enzymatic 59 (2009) 9–21.
[8] A. Saeed, S. Zaib, A. Pervez, A. Mumtaz, M. Shahid, J. Iqbal, Med. Chem. Res. 22 (2013) 3653–3662.
[9] M.A.S. Aslam, S.-U. Mahmood, M. Shahid, A. Saeed, J. Iqbal, Eur. J. Med. Chem. 46 (2011) 5473–5479.
[10] Y. Li, Z. Zhang, K. Jin, Q. Peng, W. Ding, J. Liu, Acta Chim. Sinica-Chin. Ed. 65 (2007) 834.
[11] C. Sun, H. Huang, M. Feng, X. Shi, X. Zhang, P. Zhou, Bioorg. Med. Chem. Lett. 16 (2006) 162–166.
[12] F. Wang, Z. Qin, Q. Huang, Frontiers Chem. China 1 (2006) 112–114.
[13] T. Venkatachalam, F. Uckun, Synth. Commun. 35 (2005) 2039–2056.
[14] A. Gopalsamy, H. Yang, J. Comb. Chem. 2 (2000) 378–381.
[15] F. Lieb, U. Philipp, Chem. Plant Prot. 10 (1994) 7189–7216.
[16] V. Carcu, M. Negoiu, T. Rosu, S. Serban, J. Therm. Anal. Calorim. 61 (2000) 935–945.
[17] M. Schuster, Fresen, J. Anal. Chem. 342 (1992) 791–794.
[18] W. Wasiak, J. Chromatogr. A. 690 (1995) 93–102.
[19] C. Pesco, E.A. de Campos, C.M.M. Costa, Microchim. Acta 127 (1997) 229–232.
[20] L. Nie, Z. Li, J. Han, X. Zhang, R. Yang, W.-X. Liu, F.-Y. Wu, J.-W. Xie, Y.-F. Zhao, Y.-B. Jiang, J. Org. Chem. 69 (2004) 6449–6454.
[21] P.C. Nair, M.E. Sobhia, Eur. J. Med. Chem. 43 (2008) 293–299.
[22] C. Boga, L. Forlani, C. Silvestroni, A. Corradi, P. Sgarabotto, J. Chem. Soc. Perkin Trans. 1 (1999) 1363–1368.
[23] Y. Dong, T.K. Venkatachalam, R.K. Narla, V.N. Trieu, E.A. Sudbeck, F.M. Uckun, Bioorg. Med. Chem. Lett. 10 (2000) 87–90.
[24] F. Azam, I.A. Alkskas, M.A. Ahmed, Eur. J. Med. Chem. 44 (2009) 3889–3897.
[25] M.K. Rauf, D. Imtiaz ud, A. Badshah, M. Gielen, M. Ebihara, D.d. Vos, S. Ahmed, J. Inorg. Biochem. 103 (2009) 1135–1144.
[26] D.T. Nguyen, T.H. Le, T.T.T. Bui, Eur. J. Med. Chem. 60 (2013) 199–207.
[27] http://www2.nbcr.net/data/sw/hosted/nnscore/.
[28] M. Weatherburn, Anal. Chem. 39 (1967) 971–974.
[29] M.I. Choudhary, A. Begum, A. Abbaskhan, S.G. Musharraf, A. Ejaz, Chem. Biodiversity 5 (2008) 2676–2683.
[30] P. Labute, 2007 Protonate 3D: <http://www.chemcomp.com/journal/proton.htm>.
[31] MOE (The Molecular Operating Environment) Version 2010.10, Chemical Computing Group Inc. <http://www.chemcomp.com>.
[32] D.A. Case, T.E. Cheatham, T. Darden, H. Gohlke, R. Luo, K.M. Merz, A. Onufriev, C. Simmerling, B. Wang, R.J. Woods, J. Comput. Chem. 26 (2005) 1668–1688.
[33] B. Kramer, M. Rarey, T. Lengauer, Proteins: Struct., Funct., Bioinf. 37 (1999) 228–241.
[34] http://www.biosolveit.de/LeadIT/.